Int J Pharma Res Health Sci. 2018; 6 (1): 2129-42
DOI:10.21276/ijprhs.2018.01.09
Krishnamurthy *et al*
CODEN (USA)-IJPRUR, e-ISSN: 2348-6465

PHS Scientific House
PHARMAHEALTHSCIENCES

International Journal of Pharma Research and Health Sciences

Available online at www.pharmahealthsciences.net

Original Article

Synthesis, Spectral, Thermal, Docking and Biological Activities Studies on Novel 1,4-*bis*(5-Phenylmethionone-benzimidazole)benzene and their Transition Metal Complexes.

Sunil Kumar N [1], Krishnamurthy G [1,*], Yadav D Bodke [2], Jithendra Kumara K S [1], Bhojya naik H S[2], Madhusudana somegowda [3]

[1]Department of Chemistry, Sahyadri Science College, Shimoga, Karnataka, India.
[2]Department of Industrial Chemistry, Kuvempu University, Shimoga, Karnataka, India.
[3]Department of Bio-Chemistry, Sahyadri Science College, Shimoga, Karnataka, India

ARTICLE INFO

Received: 17 Dec 2017
Accepted: 15 Jan 2018

ABSTRACT

A novel 1,4-*Bis*(5-Phenylmethionone-benzimidazole)benzene and its series of their 3d metal complexes have been synthesized in good yields. The structure was characterized by IR, uv-visible, ^{1}H-NMR, ^{13}C-NMR, Maldi mass and TGA techniques. ^{1}H NMR and ^{13}C NMR clearly shows that plane of symmetrical structure of the bis-benzimidazole ligand. IR spectra data indicate the bidentate bonding mode of ligand with 3d metal and electronic absorption spectra suggest the octahedron geometry of the Fe, Co, Ni and Cu metal complexes. The ^{1}H NMR and Maldi mass spectral data indicate tetrahedral geometry for Zn(II) complex. The antimicrobial activity of all of the synthesized compounds were evaluated against six bacterias (*Staphylococcus aureus, Staphylococcus epidemidis* , *Bacillus cereus*, *P.aeruginosa, Vibrio cholerae* and *E. coli*) and two phytopathogens fungi (*Aspergillus aureus* and *Aspergillus fumigates*) using standard method. The synthesized ligand and metal complexes are exposed to molecular docking studies using gtlucosamine-6-phosphate synthase (EC 2.6.1.16) as target site. All the synthesized compounds showed very good binding scores, among them the Zn(II) complex has more negative binding energy suggesting that, it can be a good inhibitor of glucosamine-6-phosphate synthase and is potential to act as good antimicrobial agent. The In vitro antimicrobial activity at MIC level showed that the Co(II) metal complex also exhibit potent antimicrobial activity as similar to Zn(II) complex. The complexes showed significant antioxidant activity compared to uncoordinated ligand. Among the studied complexes, zinc complex exhibited promising antioxidant activity as compared with other complexes.

KEYWORDS: Synthesis, 1,4-*Bis*(5-Phenylmethionone-benzimidazole)benzene, Metal complexes, Antimicrobial activities, Molecular docking studies, MIC level. Antioxidant activity.

1. INTRODUCTION

The drug resistance property of bacteria and fungi becoming a major worldwide problem. It is therefore need to design a suitable potent drug that overcome this resistance has

Corresponding author *
Krishnamurthy G
Department of Chemistry, Sahyadri Science College, Shimoga, Karnataka-577203
E mail: gkmnaiksahyadri@gmail.com

become one of the most important area of research today [1]. Benzimidazole derivatives are structural isosteres of naturally occurring nucleotides, which allow them to easily interact with the biopolymers of the living systems and exhibit different kinds of biological activity.

The benzimidazole ring can be substituted at the 4, 5, 6 or 7-positions, by various groups. This not only allows the introduction of other functional groups, which can be used for targeting biomolecules, but can have a major effect on the electronic properties, with a consequent influence on the SAR activity. Benzimidazole is a versatile pharmacophore producing a diverse range of biological activities including anti-inflammatory and analgesic [2-4], anti-ulcer [5], anti-fungal [6], anti-microbial [7-9], anthelmintic [10], anti-cancer [11], anti-asthmatic and anti-diabetic [12], anti-tubercular [13], antiprotozoal [14], antiviral activities etc., The optimization of benzimidazole derivatives based on their structures has resulted in various potent drugs that are now being currently practiced in the market, like albendazole, omeprazole, mebendazole, etc. Despite a numerous attempts to develop new structural prototype in the search for more effective antimicrobials, the benzimidazoles still remain as one of the most versatile class of compounds against microbes [15-22], some important benzimidazole moieties are shown below.

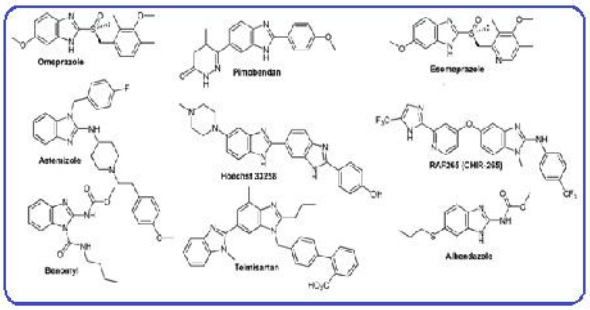

Fig 1: Clinically used benzimidazoles from the current literature.

Metal complexes of biologically vital ligands are often more active than the free ligands [23]. The biologically active heterocyclic compounds containing the benzimidazole moieties as well and their transition metal complexes were reported [24-26]. The interaction phases and the geometric position of the transition metal in ligand chelation environment serve as models to enzyme containing metal ion [27].

In this context, an attempt has been made to synthesize a pharmacological active new derivative 1,4-*Bis*(5-Phenylmethionone-benzimidazole)benzene and their metal complexes. The antimicrobial activity, molecular docking and the In-vitro antioxidant scavenging activity of uncoordinated ligand and their metal complexes have been evaluated.

2. MATERIALS AND METHODS

2.1. General Experiments

3,4-Diaminobenzophenone, terephthalic acid, LR grade orthophosphoric acid, absolute ethanol and metal salts were procured from Sigma-Aldrich (INDIA), Himedia (INDIA), Labo Chemicals(INDIA) (Commercially available from local sources) were used as received without further purification. Freshly distilled solvents were employed for all synthetic purposes. Spectroscopic grade solvents were employed for spectral works. All other chemicals were of AR grade. The progress of every coupling reaction was monitored by TLC. Yields refer to isolated yields after column chromatographic purification of compounds that have a purity of $\geq 97\%$.

The products of these reactions were authenticated by matching spectroscopic data of the products obtained with those of the reported in the literature. ^{1}H and ^{13}C NMR spectra recorded on Bruker 400 MHz spectrometer at Sophisticated Analytical Instruments Facility, Cochin University, Cochin, Kerala, India. The chemical shifts have been proven in δ values (ppm) with tetramethylsilane (TMS) as an internal standard. The signals are designated as follows: s, singlet; d, doublet; t, triplet and m, multiplet. Elemental analyses were carried out with a Perkin-Elmer 2400 Series II C, H, N analyzer. Molecular weights of unknown compounds were characterized by Electrospray ionization (Maldi-tof-ms (+ve or –ve mode)) Indian Institute of Scientific Education & Research , Pune (IISER). Uv-vis spectra recorded on varian, cary 5000. Melting points were determined in an electrically heated apparatus by taking the sample in a glass capillary sealed at one end. The Fourier transform infrared (FT-IR) spectra of the compounds were taken as KBr pellet (100 mg) the usage of a Shimadzu Fourier Transform Infrared (FT-IR) spectrometer. Reactions were monitored by thin layer chromatography on 0.25mm silicagel plates, visualized under UV light and $KMnO_4$ staining. The thermal gravimetric analysis of all metal complexes was taken by the Diamond TG/DT Analyzer (TG/DTA) at room temperature of 600 °C below on the heating rate of 20 °C min^{-1}.

2.2. Synthesis of *1,4-Bis(5-Phenylmethionone-benzimidazole)benzene (BPBB)*

3,4-Diaminobenzophenone (2 g, 9.4 mmol) and benzene-1,4-dicarboxylic acid (0.78 g, 4.7 m mol) were suspended in ortho phosphoric acid (30mL) in an 100mL round bottom flask, the resulting mixture was stirred at room temperature for 60-90 min and refluxed at 190 –195 ºC for 6 h (Scheme 1). The reaction was monitored by TLC (ethylacetate : n-hexane). After completion of the reaction, the solution was quenched into cracked ice, the resulting mass was neutralized by dilute ammonia solution, the greenish coloured precipitate was collected by filtration. The raw product was on purification by column chromatography afforded a light yellow powder final product. The probable mechanisms of reaction is shown in the scheme 2. The melting point of the product was 172 – 176 ºC. Yield: 55 %. Elemental analysis (%) found (Calculated) for $C_{34}H_{22}N_4O_2$:

C - 78.75 (77.61), H - 4.28 (3.98), N -10.80 (10.22), O - 6.17 (5.99). M_r ($C_{34}H_{22}N_4O_2$) = 518.56 g/mol. Moldy-MS in $CDCl_3$ (positive): m/z 519.17. IR (KBr, cm^{-1}): 3237 (ν -NH), 1640 (ν C=O), 1601 (ν Ar-C=N), 1534 (ν Ar-C=C), 1278 (ν Ar-C-N). M_r ($C_{34}H_{22}N_4O_2$) = 518.56 g/mol. ^1H NMR ($CDCl_3$, 400 MHz): δ = 8.085 (2H, s, H_1), 8.048-8.030 (2H, t, $J_{H30,\ H38}$ = 7.2), 7.966-7.962 (4H, d, $J_{H28,\ H32,\ H38,\ H40}$ = 1.6 Hz), 7.758-7.753(4H, d, $J_{H11,\ H12,\ H14,\ H15}$ = 2 Hz), 7.504-7.498(4H, t, $J_{H29,\ H31,\ H37,\ H39}$ = 2.4 Hz),7.449-7.447 (2H,d, $J_{H7,\ H27}$ = 0.8 Hz, H_7, H_{27}), 7.439-7.433(2H, d, $J_{H6,\ H23}$ = 2.4 Hz) 7.396 (2H, s, H_9, H_{26}). ^{13}C NMR ($CDCl_3$, 100.62 MHz): δ =197.0 (C_{16} , C_{33}), 151.6 (C_2 , C_{18}), 138.3 (C_5 , C_{20}), 132.33 (C_{27}, C_{35}), 132.11 (C_4, C_{21}), 130.75 (C_{30}, C_{38}), 130.27 (C_8, C_{25}), 130.03 (C_{10}, C_{13}), 129.70 (C_{32}, C_{36}), 129.30 (C_{28}, C_{40}), 129.17 (C_{29}, C_{39}), 129.11 (C_{31}, C_{37}), 128.22(C_{11}, C_{12}, C_{13}, C_{14}), 126.60 (C_7, C_{24}), 125.46 (C_9, C_{26}), 123.46(C_6, C_{23}). Uv-vis: λ_{max} in (nm): Δ 27397 (365 nm).

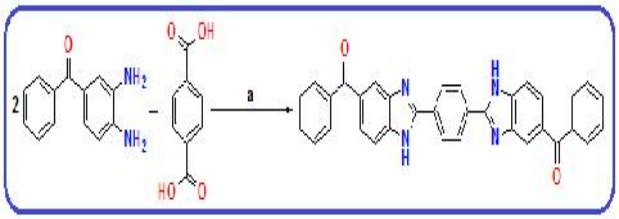

Scheme 1: Reagents and condition (a) OPA / 190–195 °C

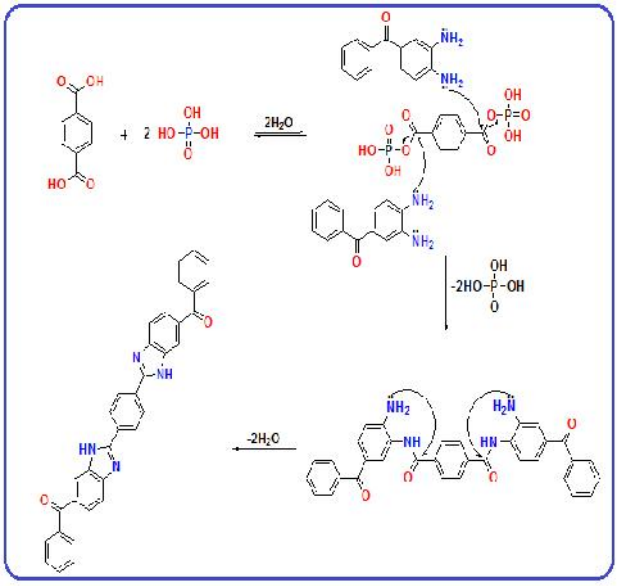

Scheme 2: The probable mechanism of cyclocondensation of 1,4-*Bis*(5-Phenylmethionone-benzimidazole) benzene using orthophosphoric acid as cyclodehydrating agent.

2.3. Synthesis of Metal Complexes.

2.3.1. Synthesis of $[Fe(BPBB)_2Cl_2]$

An ethanolic solution of $FeCl_2.6H_2O$ (62.54mg, 0.38 mmol) was mixed with a hot stirring ethanolic solution of the BPBB (0.4g, 0.77 mmol) (Fig 2). The mixture was stirred with heating for 6 h, the solid precipitated, evaporated to dryness under vacuum to give brown colored solid. The solid product was recrystallized from the methanol and the obtained complex were kept in a vacuum desiccator. The melting point of the product was 185 - 189 ºC. Yield: 69 %. Elemental analysis (%) found (Calculated) for $C_{68}H_{44}Cl_2FeN_8O_4$: C - 70.17 (69.91), H - 03.81 (03.75), Cl - 06.09 (05.89), Fe - 04.80 (04.74), N - 09.63(09.54), O - 05.50 (05.49). M_r ($C_{68}H_{44}Cl_2FeN_8O_4$) = 1164.88 g/mol. Moldy-MS in $CDCl_3$ (positive): m/z 1164.88. IR (KBr, cm^{-1}): 3383 (ν -NH), 1655 (ν C=O), 1625 (ν Ar-C=N), 1565 (ν Ar-C=C), 1285 (ν Ar-C-N), 525 (ν Metal- oxygen), 482 (ν Metal-Nitrogen). Uv-vis: λ_{max} in (nm): Δ 20618 (485 nm), Δ 24096 (415 nm).

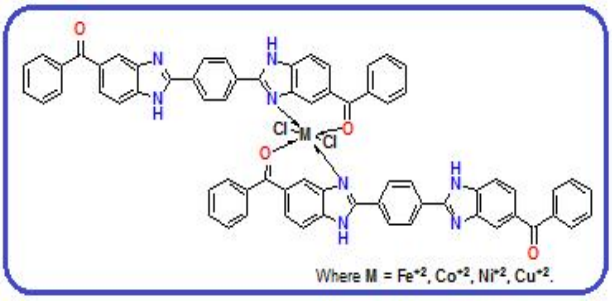

Fig 2; The structure of metal complex containing BPBB ligand.

2.3.2. Synthesis of $[Co(BPBB)_2Cl_2]$

A similar procedure was adopted for the synthesis of Co^{+2} complex ($CoCl_2.H_2O$, 90.41mg, 0.38 mmol) with ligand solution, gives light blue coloured solid. The melting point of the product was 189 – 192 ºC. Yield: 76 %. Elemental analysis (%) found (Calculated) for $C_{68}H_{44}Cl_2CoN_8O_4$: C - 69.99 (69.84), H - 03.80 (03.77) , Cl - 06.08 (05.69), Co - 05.05 (04.93), N - 09.60 (09.58), O - 05.48 (05.40). M_r ($C_{68}H_{44}Cl_2CoN_8O_4$) = 1166.97 g/mol. Moldy-MS in $CDCl_3$ (positive): m/z 1166.97. IR (KBr, cm^{-1}): 3441 (ν -NH), 1657 (ν C=O), 1621 (ν Ar-C=N), 1544 (ν Ar-C=C), 1281 (ν Ar-C-N), 561 (ν M-O), 479 (ν M-N). Uv-vis: λ_{max} (nm): Δ 14925 (670 nm), Δ18518 (540 nm).

2.3.3. Synthesis of $[Ni(BPBB)_2Cl_2]$

A similar procedure was adopted for the synthesis of Ni^{+2} complex ($NiCl_2.6H_2O$, 90.32mg, 0.38 mmol) with ligand solution, gives light green coloured solid. The melting point of the product was 187 – 193 ºC. Yield: 63 %. Elemental analysis (%) found (Calculated) for $C_{68}H_{44}Cl_2NiN_8O_4$: C - 70.00 (69.94) , H - 03.80 (03.72), Cl - 06.08 (05.78), Ni - 05.03 (04.98), N - 09.60 (09.58), O - 05.49 (05.37). M_r ($C_{68}H_{44}Cl_2NiN_8O_4$) = 1166.73 g/mol. Moldy-MS in $CDCl_3$ (positive): m/z 1166.73. IR (KBr, cm^{-1}): 3372 (ν -NH), 1648 (ν C=O), 1619 (ν Ar-C=N), 1570 (ν Ar-C=C), 1285 (ν Ar-C-N), 513 (ν M-O), 488 (ν M-N). Uv-vis: λ_{max} (nm): Δ 12345 (810 nm), Δ 14492 (690 nm), Δ 22727 (440 nm).

2.3.4. Synthesis of the $[Cu(BPBB)_2Cl_2]$.

Synthesis of this complex was done by following the procedure used for the synthesis of $[Fe(BPBB)_2Cl_2]$. The addition of ethanolic solution of $CuCl_2.2H_2O$ to a hot ethanolic solution of the BPBB, which gives a dark green coloured solid. The melting point of the product was 189 –

196 ºC. Yield: 67 %. Elemental analysis (%) found (Calculated) for $C_{68}H_{44}Cl_2CuN_8O_4$: C - 69.71(69.69), H - 03.79 (03.77), Cl - 06.05 (05.91), Cu - 05.42 (05.38), N - 09.56 (09.55), O - 05.46 (05.35). M_r ($C_{68}H_{44}Cl_2CuN_8O_4$) = 1166.73 g/mol. Moldy-MS in $CDCl_3$ (positive): m/z 1166.73. IR (KBr, cm^{-1}): 3243 (ν -NH), 1642 (ν C=O), 1607 (ν Ar-C=N), 1539 (ν Ar-C=C), 1285 (ν Ar-C-N), 525 (ν M-O), 492 (ν M-N).). Uv-vis: λ_{max} (nm): Δ 15151 (660 nm).

2.3.5. Synthesis of [Zn(BPBB)Cl_2]

A solution of $ZnCl_2$ (0.09g, 0.77mmol)in ethanol was prepared and mixed with a hot stirring ethanolic solution of the BPBB (0.4g, 0.77 mmol) (Fig 3). The resulting solution was heated with stirring about 6 h, the pale yellow solution was obtained which was evaporated slowly to remove excess of solvent. The solid was recovered by filtration and recrystallized from methanol. The obtained complex were kept in a vacuum desiccator. The melting point of the product was 179 – 184 ºC. Yield: 61 %. Elemental analysis (%) calculated (found) for $C_{68}H_{44}Cl_2CuN_8O_4$: C - 62.36 (62.27), H - 03.39 (03.33), Cl - 10.83 (10.72), Zn - 09.99 (09.89), N - 08.56 (08.45), O - 04.89 (04.76). M_r ($C_{34}H_{22}Cl_2ZnN_4O_2$) = 654.86 g/mol. Moldy-MS in $CDCl_3$ (positive): m/z 654.86. IR (KBr, cm^{-1}): 3242 (ν -NH), 1643 (ν C=O), 1607 (ν Ar-C=N), 1541 (ν Ar-C=C), 1285 (ν Ar-C-N), 530 (ν M-O), 495 (ν M-N).

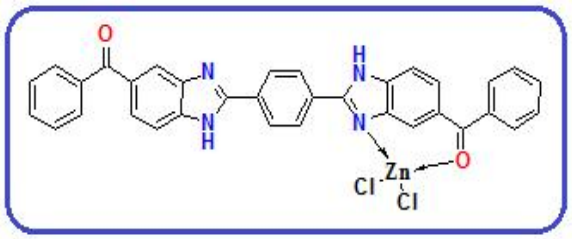

Fig 3: The structure of zinc metal complex containing BPBB ligand

2.4. Antimicrobial activity.

2.4.1. Antibacterial screening.

The antibacterial activity of the compounds were tested against gram positive bacteria namely *staphylococcus aureus*, *staphylococcus epidemidis* and *bacillus cereus* and gram negative bacteria namely *pseudomonas aeruginosa*, *vibrio cholerae* and *escherichia coli* by agar well diffusion method. Twenty four old Muller-Hinton broth cultures of test bacteria were swabbed on sterile Muller-Hinton agar plates using sterile cotton swab followed by punching wells of 6mm with the help of sterile cork borer. The standard drug (chloramphenicol, 100 µg/mL of sterile distilled water), three different concentrations (100, 50 and 25 µg /mL in 10% DMSO) and control (10% DMSO) were added to respective labeled wells. The plates are allowed to stand for 30 min. and were incubated at 37 ºC for 24 h in upright position and the zone of inhibition was recorded [28]. During this period, the test solution diffused and zone of inhibition were recorded using vernier callipers.

2.4.2. Antifungal screening.

Antifungal activity of the compounds was evaluated against *Aspergillus aureus* and *Aspergillus fumigates* fungus, using the sabouraud dextrose agar diffusion method [29]. Wells were made (6mm diameter) with a sterile cork borer. The standard drug (Fluconazole, 100 µg/mL of sterile distilled water) and control (10% DMSO) were added to respectively labeled wells. To these wells 140 µL from each (100, 50 and 25 µg/mL in 10% DMSO) of the test stock solution compounds were added and the plates were allowed to cool for an hour to facilitate the diffusion. The plates were then incubated at 37 ºC for 48 h. At the end of the incubation period, the diameter of the zone of inhibition around the wells was measured using vernier callipers.

2.5. Molecular docking studies.

Three dimensional structure of glucosamine-6-phosphate synthase (PDB Id - 2VF5) retrieved from Protein Data Bank (PDB) http://www.pdb.org of resolution 2.90 Å. The water molecule and hetero atoms were removed from the protein, the non-polar hydrogen atoms were added, followed by gasteiger charger calculation using Autodock tools. Then the structure was saved in PDBQT file format for further analysis. The lignads were drawn in ACD/ChemSketch 2015.2.5 with proper 2D orientation and energy minimization was carried out using Dundee PRODRG2 server (Schuttelkopf and Aalten, 2004) and saved in PDBQT file format. Molecular docking studies were carried out using Autodock Vina Program with grid box of size set at 70, 64 and 56 Å for x, y and z respectively, which centered on mass center 30.59, 15.822 and -3.497 for x, y and z respectively of the crystallographic macromolecule covering all active site atoms (Thr 302, Ser 303, Cys 300, Gly 301, Ser 347, Gln 348, Ser 349, Ala 400, Val 399, Ala 602, Lys 603 Thr 352,). The spacing between grid points was 1 Å. The output result were analyzed with Ligplot and Pymol.

2.6. Antioxidant activity.

This activity for the synthesized compounds were performed using DPPH method as per literature [30]. The compounds of different concentrations are dissolved in menthaol and were introduced to each vials of 5mL. To this test vials 3 mL of 0.004% DPPH in methanol was added and the mixtures have been incubated in dark condition at ambient temperature for 30 min. Ascorbic acid is used as the standard. The absorbance reduced while the DPPH is scavenged by way of an antioxidant, through contribution of hydrogen to shape a strong DPPH molecule. DPPH scavenging activity calculated by the use of the following equation and absorbance measured at 517 nm.

Scavenging ratio (%) = [(Ai–Ao)/(Ac–Ao)] × 100%

Where

Ai is the absorbance within the presence of the check compound.

Table 1 : Analytical and physical properties of BPBB and their metal complexes.

Entry	Compounds	Mol. wt	Yield %	C, H, N, O and Metal (%) Analysis found (calculated)						Ohm/Cm^2/mol
				M	C	H	N	O	Cl	
1	L (Light yellow)	518.56	45	---	78.75	04.28	10.80	06.17	---	---
2	[$FeCl_3L_2$] (Light Brown)	1163.88	78	04.80	70.17	03.81	09.63	05.50	06.09	12.71
3	[$CoCl_2L_2$] (Light blue)	1166.97	83	05.50	69.99	03.81	09.60	05.48	06.08	12.88
4	[$NiCl_2L_2$] (Light green)	1166.73	75	05.03	70.00	03.80	09.60	05.49	06.08	17.58
5	[Cu L_2Cl_2](Dark green)	1171.58	76	05.42	69.71	03.79	09.56	05.59	06.05	15.58
6	[$ZnCl_2L$](Pale yellow)	654.87	81	09.99	62.36	03.39	08.56	04.89	10.83	04.29

Ao is absorbance of the clean inside the absence of the check compound.

Ac is the absorbance within the absence of the test compound.

3. RESULTS AND DISCUSSION

3.1. Chemistry.

The majority of research articles focusing on cyclization of o-phenylenediamine with aromatic acids to form benzimidazole ring in the presence of Bronsted-Lowry acid 6N HCl [31] or strong dehydrating agent polyphosphoric acid (PPA) [32-33] as solvents, fortunately in case of dicarboxylic aromatic acid like 1,4-dicarboxylic acid the cyclization of o-phenylenediamine will not be achieved. It is therefore setup new way to synthesize *bis*-benzimidazole by using ortho-phosphoric acid (OPA), a strong cyclodehydrating agent. Heating the 3,4-diaminobenzophenone with 1,4-dicarboxylic acid in OPA solvent at 190–195 ºC for 6 h afforded a symmetrical structured BPBB in moderate yield (Scheme-1). The reaction probably proceeds via the mechanism illustrated in Scheme 2. The 1,4-*bis*(5-Phenylmethionone-benzimidazole)benzene were characterized by elemental analysis, IR, ^{1}H NMR, ^{13}C NMR and mass spectral data.

The complexes were prepared by the reaction of the hot alcoholic solution of ligand (BPBB) with the alcoholic solution of metal chlorides (M = Fe(II), Co(II), Ni(II), Cu(II) and Zn(II)) in methanol. All compounds are stable under atmospheric conditions and are soluble in polar organic solvents like DMF, DMSO, MeCN and partially soluble in methanol, water, ethylacetate and chloroform. Insoluble in Et_2O and petroleum ether. The elementary analysis of the complexes of Fe(II), Co(II), Ni(II) and Cu(II) showed that the metal and ligand are in 1:2 molar ratio and the complex of Zn(II) are in 1:1 molar ratio. The elemental analyses of the complexes were consistent with the calculated results from the empirical formula of each complexes represented in Table 1. The molar conductivities of 10^{-3} M of the complexes (dissolved in DMF) at room temperature were measured, the results are in the range 04.29–17.58 $\Omega^{-1}mol^{-1}cm^2$ for all the complexes. The slightly higher values observed may be due to partial dissociation of the complexes in DMF solvent [34-35]. The compounds were characterized on the basis of the following studies.

3.2. IR spectra and mode of bonding.

The infrared spectra data of the BPBB ligand and its metal complexes are summarized in table 2 and fig 4. The IR spectraum of the ligand and complexes were recorded in the region of 4000 – 400 cm^{-1}. The free ligand BPBB displayed characteristic (ν N–H) stretching band at 3237 cm^{-1}, a medium intensity band at 1458 cm^{-1} and 1278cm^{-1} assigned to (ν C=N) and (ν C–N) of the imidazole moiety respectively and due to the extended conjugation ligand showed a sharp band at 1640 cm^{-1} for (ν C=O) and the aromatic (ν C=C) stretching band shown at 1534 cm^{-1}.

In the complexes, the band due to (ν N–H) remains unaltered excepting some slight variation in the position indicating non-participation of N-H group in complex formation. The effect of metal ions on binding modes has been investigated. The observed bands at 1458cm^{-1} were assigned as ring stretching, ring bending and ring out of plane deformation respectively [36-41]. These bands were shifted by 3 - 23 cm^{-1} towards high frequencies upon complexation with metal ions. The skeletal modes of these intra molecular vibrations should be hindered by the effect of metal ions, which bind the benzimidazolyl nitrogen. Slight higher frequency shift of (ν C=N) vibrations appear in the region 1458cm^{-1}-1486 cm^{-1} for all the metal complexes and stretching bands observed around 472 cm^{-1} to 495 cm^{-1} in metal complexes, these absorptions support the argument that coordination most probably occurs through imine nitrogen atoms of benzimidazole [42]. The position of (ν C=O) band is shifted to the higher frequencies in the region between 1657-1642 cm^{-1} in the spectrum of the metal complexes, indicating that the coordination occurs through the oxygen atom of carbonyl carbon of BPBB to the metal ion. The stretching bands observed around 584 cm^{-1} to 560 cm^{-1} in metal complexes indicating (ν M-O) mode of bonding [43-44].

Table 2 : FTIR spectral data (cm^{-1}) of BPBB and its metal complexes.

Entry	Compounds	N-H	C=C (Ar)	C=N (Ar)	C=O	C-N	Others
1	Ligand	3237	1534	1601	1640	1278	
2	$[Fe(BPBB)_2Cl_2]$	3383	1565	1625	1655	1285	M-N = 482 M-O = 525
3	$[Co(BPBB)_2Cl_2]$	3441	1544	1621	1657	1281	M-N = 479 M-O = 561
4	$[Ni(BPBB)_2Cl_2]$	3372	1570	1619	1648	1285	M-N = 488 M O = 531
5	$[Cu(BPBB)_2Cl_2]$	3243	1539	1607	1642	1285	M-N = 492 M-O = 525
6	$[ZnCl_2(BPBB)]$	3242	1541	1607	1643	1285	M-N = 495 M O = 530

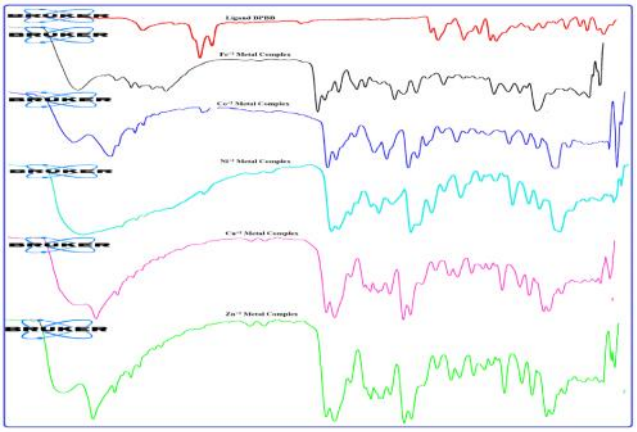

Fig 4: FT-IR Spectra of Ligand BPBB and its Metal complexes.

3.3. ^{1}H NMR and ^{13}C NMR spectra.

The ^{1}H NMR spectra of the BPBB compound were obtained in $CDCl_3$ solvent at room temperature using TMS as an internal standard. The ^{1}H NMR spectrum of the BPBB showed a singlet peak which is attributed to imidazole -NH at 8.08 ppm and a multiplet in the range 8.04 - 7.20 ppm for both imidazole and aromatic benzene nuclei protons which are shown in fig 5. The ^{13}C NMR spectrum of the BPBB showed a signal at 197.0 ppm for (C=O) group and a signal at 151.6 ppm is assigned to (N-C=N). The peaks in the region 138.2 - 123.0 ppm are due to aromatic carbons which confirming the structure of the ligand and is showed in fig 6. The ^{1}H NMR spectrum of Zn(II) complex were obtained in DMSO solvent, it represented in fig 7. The aromatic protons from 7.986 - 7.203 ppm for imidazole and benzene rings are shifted to slight upper field due to the increased conjugation on coordination. The signal due to -NH at 8.203 ppm appeared with slight shift towards down field indicates no participation of -NH group in the coordination.

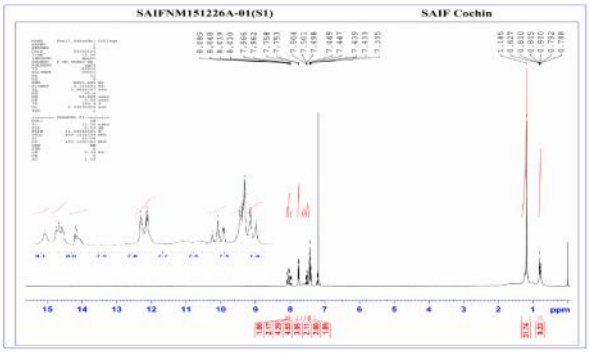

Fig 5: ^{1}H NMR spectrum of the BPBB ligand

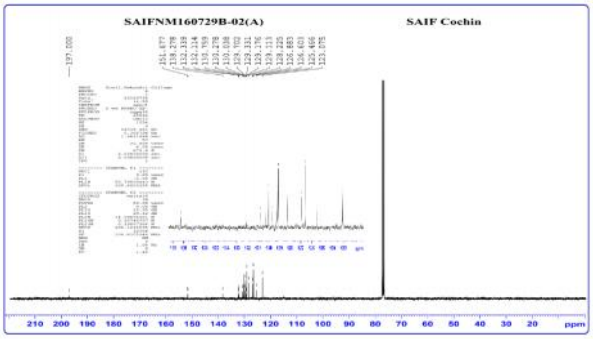

Fig 6: ^{13}C NMR spectrum of the BPBB ligand.

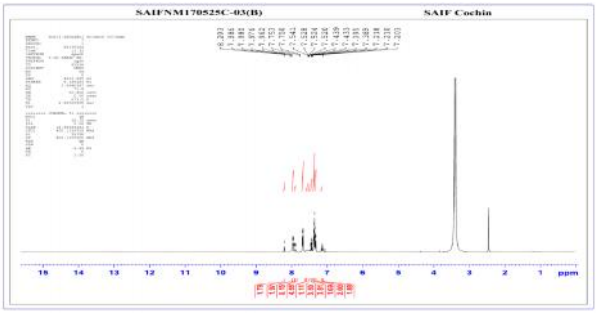

Fig 7: ^{1}H NMR spectrum of the Zn^{+2} metal complex.

3.4. Mass spectra.

The electrospray ionization (ESI) mass spectral investigation of BPBB is in good agreement with its calculated values and is presented in fig 8. The compound give a molecular ion peak at m/z 519 with characteristics isotopic contribution. The m/z value 415 and 222 indicating respective cleavage of the benzilic carbonyl and benzene ring of BPBB ligand. On fragmentation, one side of the ligand is removed yielding a base peak at 299, indicating the most stable skeletal system of the ligand. Thus the molecular ion peak and the base peak of the ligand are obtained at 519 and 299 respectively. The mass spectrum Zn(II) complex gave a molecular ion peak at m/z 654.62 (M+2 Peak 655.60) which indicate that metal:ligand is in 1:1 ratio as in fig 9.

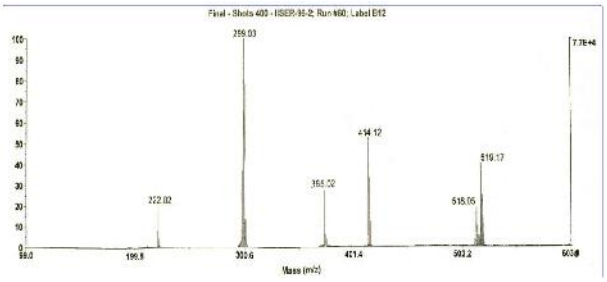

Fig 8: Maldi mass of the BPBB ligand

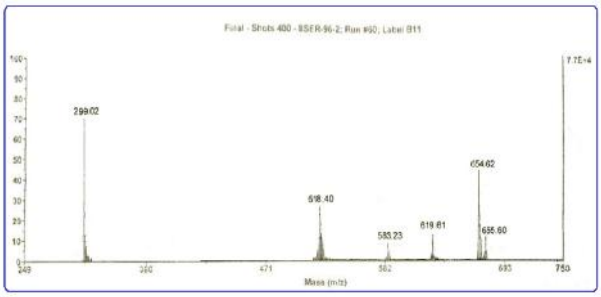

Fig 9: Maldi mass of the Zn^{+2} metal complex.

3.5. Electronic absorption spectra.

In order to understand the physicochemical properties of metal complexes, it is important to know the electronic structure of ligand and metal complexes. The electronic absorption spectrum of ligand and metal complexes were recorded in DMSO solvent in the range 250 - 900 nm and the data were presented in table 3 and fig 10. The spectrum of BPBB displayed three absorption bands in DMSO solvent. The first and second bands at Δ_1=38461cm^{-1} and Δ_2=35087cm^{-1} may be assigned to π → π* transitions in the delocalized π-electron. The longer wavelength band at Δ_3=27027cm^{-1} can be assigned to an intramolecular charge transfer interaction from the aromatic nucleus to the neighboring nitro acceptor center [45]. The electronic absorption spectrum of Fe (II) metal complex showed two absorption bands at Δ_1 = 24390 cm^{-1} and Δ_2 = 20833 cm^{-1} in DMSO are assigned to the $^5T_2g(D) \rightarrow {}^5E_g(D)$ ($\upsilon_{1)}$ transitions. This band is a composite of the splitting of the excited state energy level ^5E_g into two non-degenerate energy levels, which form a characteristic transition band in iron complex. The other expected bands are not properly appeared in the spectrum. The Fe(II) complex showed the magnetic moment of 4.9 BM, hence the complex is expected to have octahedral geometry. The Co(II) complex exhibited two absorption bands. A band occure at Δ_1=15037 cm^{-1} and the another higher energy band at Δ_2= 17543 cm^{-1} corresponding to the transition $^4T_{1g}(F) \rightarrow {}^4T_{2g}(F)$ ($\upsilon_{1)}$ and $^4T_{1g}(F) \rightarrow {}^4T_{1g}(P)$ ($\upsilon_{2)}$ respectively and the observed magnetic moment of 3.3 BM also support for the octahedral geometry [46-47]. Three absorption bands are obtained for Ni^{+2} complex in the range Δ_1=23255cm^{-1}, Δ_2=14492cm^{-1} and Δ_3=12492cm^{-1} corresponding to $^3A_{2g}$ (F) → $^3T_{1g}$ (P) (υ_1), $^3A_{2g}(F) \rightarrow {}^3T_{2g}(F)$ (υ_2) and $^3A_{2g}$ (F) → $^3T_{1g}$ (F) (υ_3) attributed to d-d electron transitions. The magnetic moment obtained is 2.6 BM, suggest the octahedral geometry. In the case of Cu(II) complex, a broad band appeared at Δ_1=15503 cm^{-1} is assigned to the transition $^2Eg \rightarrow {}^2A_{1g}$ (υ_1) and the observed magnetic moment of 1.4 BM support octahedral geometry of the complex.

Table 3 : Electronic Absorption Spectral Bands of the ligand BPBB and their Complexes

Compound	Electronic transition υ (cm^{-1})	μ_{eff} (BM)
BPBB ligand	38,461, 35,087 and 27,027	---
[Fe (BPBB)$_2$Cl$_2$]	24,390 and 20,833	4.9
[Co (BPBB)$_2$Cl$_2$]	15,037 and 17,543	3.3
[Ni (BPBB)$_2$Cl$_2$]	14,492 , 12,492 and 23,255	2.6
[Cu (BPBB)$_2$Cl$_2$]	15,503	1.1

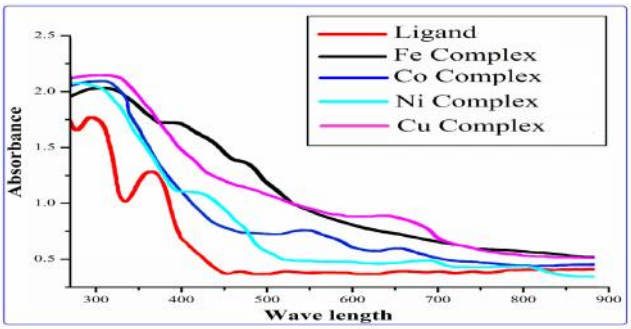

Fig 10: Electronic Absorption Spectral Bands of the ligand BPBB and their Complexes.

3.6. Thermal analyses and kinetics studies.

3.6.1. Thermal analyses.

In the present investigation, heating rates were suitably controlled at 5 ºC min^{-1} under nitrogen atmosphere and the weight loss was measured from the ambient temperature up to 600 ˚C. The data are listed in table 4 and fig 11. The thermogram of Fe(II) complex showed three decomposition in the temperature range 30 – 600 ºC. The first step of decomposition occur within the temperature range 30 – 145 ºC correspond to the loss of two coordinated chlorine atoms with a mass loss of 6.03% and the energy of activation is 2.97 kJ mol^{-1}. The subsequent steps (150 – 530 ºC) correspond to complete dissociation of the ligand for the mass loss = 88.75%, leaving FeO as residue. The Co(II) complex showed the loss of two chlorine atoms from 30 to 155 ºC with the mass loss = 6.12 %. The energy of activation for this step is 3.19 kJ mol^{-1}. The loss of ligand molecules occur with a mass loss of 88.96% in the temperature range 155- 600 ºC, leaving CoO as a residue with the total weight loss amounts to 97.10%. Similarly, the Ni(II) complex exhibits the decomposition in the temperature range 100 – 135 ºC with the mass loss = 6.08%, for the dissociation of two chlorides, with activation energy for this step is 3.71 kJ mol^{-1}. The second decomposition step occur form 135 –

605 ºC corresponding to the loss of 88.93%, due to the loss of BPBB and leaving behind NiO as residue. In the case of Cu(II) complex, the decomposition step with an estimated mass loss of 6.25% in the temperature range 90 – 130 ºC, attributed to the loss of coordinated two chlorides with the activation energy is 4.14 kJ mol^{-1}. Another decomposition step found within the temperature range 130 – 520 ºC is due to the last of BPBB with an estimated mass loss of 88.78% leaving CuO as a residue. The overall weight loss amounts to 97.19%.

Table 4 : Thermoanalytical results (TGA and DTA) of metal complexes of BPBB.

Complex	G range (°C)	TA (°C)	*	ass loss %	otal mass loss %	ssignment	etallic residue
Fe (BPBB)$_2$Cl$_2$]	0 – 145	5(+), 130(+), 180(-), 370(-), 450(-), 490(+), 520(-),535(+).		.03	4.78	oss of 2Cl$^-_2$	eO
	50 – 610			8.75		oss of organic part of the ligand	
Co (BPBB)$_2$Cl$_2$]	0 – 155	10(+), 145(+), 210(-), 320(-), 350(-, 450(+).		.12	5.08	oss of 2Cl$^-_2$	oO
	55 – 600			8.96		oss of organic part of the ligand	
Ni (BPBB)$_2$Cl$_2$]	0 – 135	7(+), 190(+), 230(-), 350(-), 425(-).		.08	5.01	oss of 2Cl$^-_2$	iO
	35 – 605			8.93		oss of organic part of the ligand	
Cu (BPBB)$_2$Cl$_2$]	0 – 130	15(+), 180(-), 290(-), 390(-), 410(+), 430(-)		.25	5.03	oss of 2Cl$^-_2$	uO
	35 – 600			8.78		oss of organic part of the ligand	

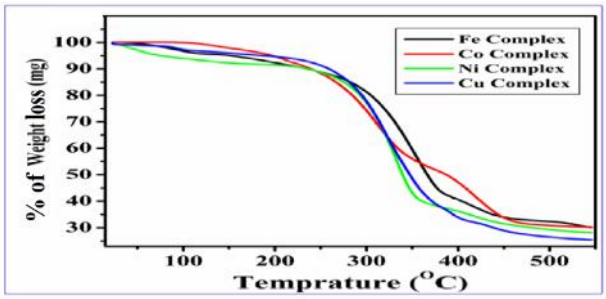

Fig 11: Thermoanalytical (TGA and DTA) of metal complexes of BPBB.

3.6.2. Kinetic studies.

The thermodynamic activation parameters of decomposition processes of dehydrated complexes namely activation energy (ΔE*), enthalpy (ΔH*), entropy (ΔS*) and Gibbs free energy change (ΔG*) of the decomposition were evaluated graphically by employing the Coats – Redfern relation [48]. The data are summarized in Table 5. The values of the activation energies reflect the thermal stability of the complexes. The activation energies of decomposition are found to be in the range 2.97 to 4.14 kJ mol^{-1}. The ΔE* is found to have negative values in all the complexes indicating that the decomposition reactions proceed with lower rate than the normal ones.

Table 5 : Thermodynamic data of the thermal decomposition of metal complexes of BPBB

Complex	Decomp. temp. (°C)	E^* (kJ mol^{-1})	ln A Min^{-1}	ΔH^* (kJ mol^{-1})	ΔS^* (kJ mol^{-1})	ΔG^* (kJ mol^{-1})
[Fe (BPBB)$_2$ Cl$_2$]	275	2.977	3.306	0.690	-154.21	42.40
	415		3.480	-0.473	-35.75	62.07
[Co (BPBB)$_2$ Cl$_2$]	240	3.193	3.457	1.197	-134.52	33.49
	405		3.484	-0.174	-150.14	60.81
[Ni (BPBB)$_2$ Cl$_2$]	217	3.718	3.813	1.910	-119.43	27.88
	330		3.530	0.974	-152.74	50.41
	435		3.724	0.101	-148.97	64.81
[Cu (BPBB)$_2$ Cl$_2$]	207	4.140	4.101	2.415	-156.61	32.50
	352		3.758	1.209	-151.68	53.46
	450		3.865	0.399	-148.50	66.82

3.7. Biological activity studies.

3.7.1. In vitro antibacterial and antifungal activity.

The data showed that the BPBB and its metal complexes have the capacity of inhibiting the metabolic growth of the investigated bacterial and fungal strains. Antimicrobial activity in different concentrations of ligand BPBB and its metal complexes were revealed in Table 6. The inhibitory activity of complexes is related to the cell wall structure of the microbs. Which is essential to the survival of bacteria. Some antibiotics are able to kill the bacteria by inhibiting the synthesis of peptidoglycan [49]. A possible explanation for the poor activity of these complexes with respect to their ligand may be attributed to their inability to chelate metals is essential for the metabolism of microorganisms and/or to form hydrogen bonds with the active centers of cell structures, resulting in an interference with the normal cell cycle. Furthermore, the low activity of these complexes may be due to their low lipophilicity, because of which penetration of the complex through the lipid membrane may decrease and hence, they could neither block nor inhibit the growth of the microorganism. Therefore, we confirm that the toxicity of the complexes can be related to the strengths of the M–L bond, size of the cation and receptor sites [50-51]. The

size of the inhibition zone depends upon the culture medium, incubation conditions, rate of diffusion and the concentration of the antimicrobial agent (the activity increases as the concentration increases). In the present study, the BPBB and its metal complex are active against the bacteria and fungi, which may indicate broad-spectrum properties. The remarkable activity of these compounds may be arising from the two benzimidazole ring, which may play an important role in the antibacterial activity. The mode of action may involve the formation of a hydrogen bond through the tertiary nitrogen of the imidazole ring with the active centers of the cell constituents, resulting in interference with the normal cell process.

As a result of this, the primary screening against the bacterial strains in different concentrations showed good zone of inhibition as shown in fig 12 and fig 13. The Co(II) complex exhibited the highest antibacterial activity against *P aeruginosa*, *V cholerae* and *S epidemidis*. The Ni(II), Cu(II) and Zn(II) complexes showed good antibacterial activity towards *B cereus*, *S aureus* and *E coli* respectively [52]. The Zn(II) complex performs highest antifungal activity against *A aureus* and *A fumigates*, the primary screening against the fungal strains in different concentrations showed good zone of inhibition as shown in fig 14 and fig 15. The ligand and Fe(II) complex showed the least activity against *B subtilis* bacteria and both fungal strains. The MIC study of both BPBB and metal complexes against bacterial and fungal strains at different concentrations i.e., 1, 10, 25, 50, and 100 µg/mL was evaluated. The MIC data of antimicrobial activity of the ligand and its metal complexes are reported in table 7. The fig 16 and 17 represents the MIC activity against bacterial and fungal strains. The Co(II) and Zn(II) complexes showed potential MIC values against bacterial and fungal strains respectively..

Table 6 : Antimicrobial activity of the isolated ligand and its metal complexes.

Compound	Concentration in µg/ml	Growth inhibition against *bacteria in mm*						Growth inhibition against *fungicides in mm*	
		P.aeruginosa	*S.aureus*	*V.cholerae*	*S.epidermidis*	*B.subtilis*	*E.coli*	*A. aureus*	*A.fumigatus*
Ligand BPBB	25	12.06±0.05	15.03±0.25	15.10±0.26	14.03±0.25	11.01±0.20	12.07±0.45	08.17±0.25	05.20±0.20
	50	14.19±0.05	16.00±0.20	16.03±0.31	15.10±0.26	11.05±0.05	13.02±0.03	12.13±0.31	06.30±0.20
	100	16.06±0.04	16.06±0.04	17.13±0.31	16.00±0.20	00.00±0.00	13.06±0.25	14.00±0.21	09.27±0.23
[Fe $(BPBB)_2Cl_2$]	25	13.10±0.18	12.17±0.22	13.32±0.20	13.25±0.15	10.11±0.17	11.26±0.17	12.11±0.17	11.14±0.15
	50	15.16±0.14	14.06±0.05	14.29±0.03	14.35±0.30	00.00±0.00	13.27±0.16	13.44±0.20	14.36±0.15
	100	17.03±0.03	16.52±0.38	17.48±0.21	16.72±0.33	00.00±0..00	16.218±0.07	15.59±0.33	17.35±0.10
[Co $(BPBB)_2Cl_2$]	25	20.19±0.13	15.27±0.08	19.26±0.06	18.34±0.34	15.37±0.24	17.14±0.12	17.17±0.16	12.48±0.10
	50	23.20±0.12	16.25±0.10	20.24±0.16	19.40±0.14	16.39±0.17	19.00±0.23	19.38±0.14	14.28±0.07
	100	28.35±0.20	20.28±0.16	24.14±0.16	24.36±0.23	21.20±0.14	20.14±0.18	21.05±0.02	21.44±0.09
[Ni $(BPBB)_2Cl_2$]	25	18.25±0.05	11.27±0.08	16.25±0.06	15.22±0.02	17.06±0.04	13.02±0.11	20.42±0.17	16.21±0.14
	50	19.26±0.04	15.06±0.05	17.26±0.04	16.45±0.04	19.31±0.06	14.20±0.20	22.35±0.20	20.36±0.25
	100	23.47±0.23	20.18±0.20	20.46±0.27	19.27±0.07	22.23±0.19	16.00±0.02	25.41±0.23	22.15±0.15
[Cu	25	16.19±0.17	19.27±0.25	16.28±0.05	14.30±0.19	16.28±0.05	14.21±0.33	18.48±0.19	15.25±0.09

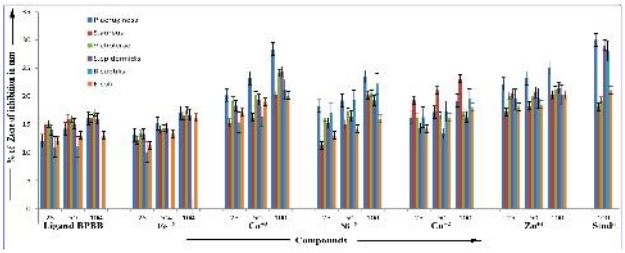

Fig 12: Antibacterial activity of the ligand and its metal complexes.

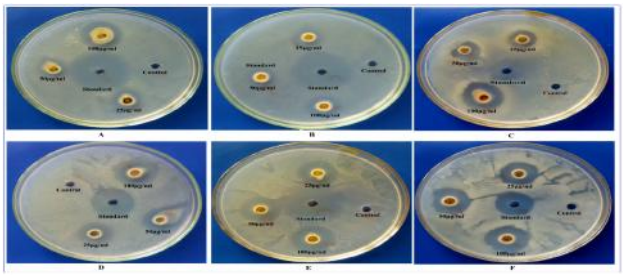

Fig 13; Antibacterial activity of the ligand and its metal complexes.

A) *Pseudomonas aeruginosa* interact with BPBB ligand B) *Escherichia coli* interact with Fe metal complex C) *Bacillus cereus* interact with Co metal complex D) *Staphylococcus epidemidis* interact with Ni metal complex E) *Staphylococcus aureus* interact with Cu metal complex F) *Vibrio cholera* interact with Zn metal complex.

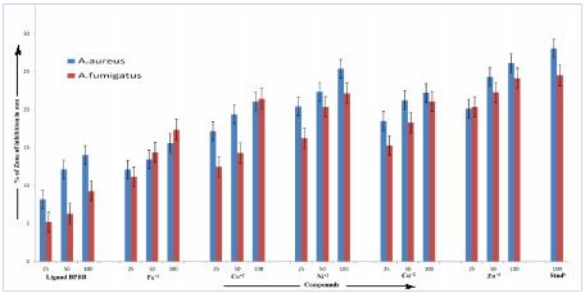

Fig 14: Antifungal activity of the ligand and its metal complexes.

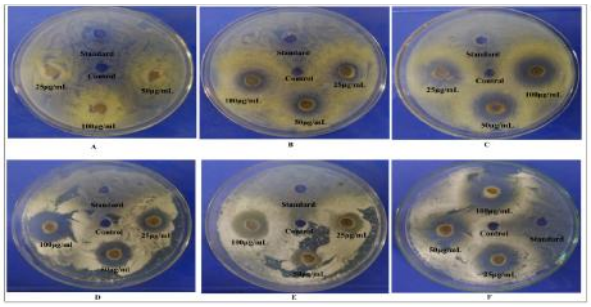

Fig 15: Antifungal activity of the ligand and its metal complexes.

A) *Aspergillus aureus* interact with BPBB ligand B *Aspergillus aureus* interact with Fe metal complex C) *Aspergillus aureus* interact with Co metal complex D) *Aspergillus fumigates* interact with Ni metal complex E) *Aspergillus fumigates* interact with Cu metal complex F) *Aspergillus fumigates* interact with Zn metal complex.

Table 7: MIC data of antimicrobial activity of the ligand and its metal complexes

Compound	Growth inhibition against *bacteria in mm*						Growth inhibition against *fungicides in mm*	
	P.aeruginosa	*S.aureus*	*V.cholerae*	*S.epidermidis*	*B.subtilis*	*E.coli*	*A. aureus*	*A.fumigatus*
Ligand BPBB	250	500	250	250	NT	500	250	NT
[Fe $(BPBB)_2Cl_2$]	500	250	500	500	NT	250	250	500
[Co $(BPBB)_2Cl_2$]	700	500	700	500	500	500	500	250
[Ni $(BPBB)_2Cl_2$]	700	250	500	500	700	500	700	500
[Cu $(BPBB)_2Cl_2$]	500	500	500	250	500	500	700	500
[$ZnCl_2$(BPBB)]	500	500	700	700	500	500	700	700
Stnd[a]	250	250	250	NT	NT	250	-	-
Stnd[b]	-	-	-	-	-	-	250	NT

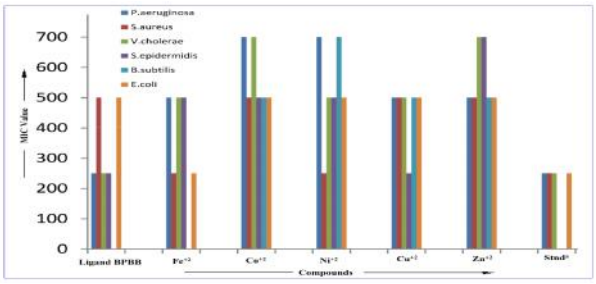

Fig 16: MIC data of antibacterial activity of the ligand and its metal complexes.

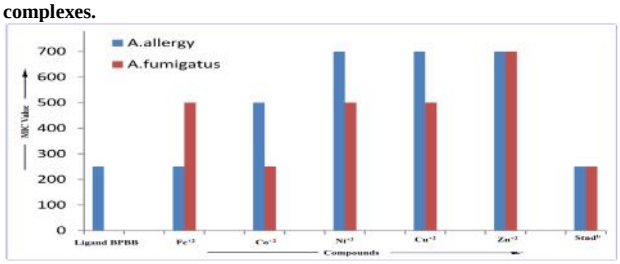

Fig 17: MIC data of antifungal activity of the ligand and its metal complexes.

3.7.2. Molecular docking studies.

L-glutamine: D-fructose-6-phosphate aminotransferase were used as a target for antimicrobial activity of the synthesized compounds as potential inhibitors. This enzyme is commonly known as Glucosamine-6-phosphate synthase (EC 2.6.1.16) belongs to enzyme class transferase. This enzyme catalyze the important step in the formation of uridine diphosphate N-acetylglucosamine (UDP-GlcNAc). Which transfer ammonia from L-glutamine to fructose-6-phosphate (Fru-6-P), and followed by isomerisation of formed fructosamine-6-phosphate to glucosamine-6-phosphate. Fungi and bacteria solely use UDP-GlcNAc to build their cell wall assembly, e.g. chitins and mannoproteins in case of fungi and peptidoglycan in bacteria. The docking simulations in the active sites of Glucosamine-6-phosphate syntheses were performed by Auto Vina program. Docking studies of synthesized BPBB and metal complexes with the enzyme showed that all of the inhibitors can bind to one or more amino acids in the active site.

Theoretically all the synthesized compounds showed very good binding scores ranging from -9.5 to -13.1 kcal/mol. Among the synthesized compounds Zn(II) showed less binding energy compared to the other compounds suggesting that it may be considered as a good inhibitor of glucosamine-6-phosphate synthase and is potential to act as a good antimicrobial agent. These results are in accordance with experimental results listed in Table 8 and showed in fig 18.

Table 8 : Docking study of synthesized BPBB ligand and metal complexes

Drug molecule	Affinity (kcal/mol)	H-Bonds	H-bond length (Å)	H-bond with Hydrophobic	Interactions
Ligand BPBB	-9.5	1	3.11	Val605	His493, Glu488,Gly301,Ser604,T

					hr3 52, Lys603, Cys300,Gln348, Ser349,Leu601, Leu484, Lys487,Tyr491
[Fe $(BPBB)_2Cl_2$]	-12.4	-	-	-	Ser328,Tyr332, Glu329
[Co $(BPBB)_2Cl_2$]	-12.0	1	3.30	Asn 305	Ala483, Leu484, Gly301, Leu480, Lys487, Ala496, Ala483
[Ni $(BPBB)_2Cl_2$]	-11.8	1	3.09	Ala602	Val605, Leu601
[Cu $(BPBB)_2Cl_2$]	-11.1	-	-	-	Tyr491, Leu601, Arg599, Ala498,Tyr476, Ala496,Tyr497, Asn600,Lys487, Tyr304, Asn305,Leu480, Glu488
[$ZnCl_2$(BPBB)]	-13.1	-	-	-	Thr352, Val605, Asp354, Ala353

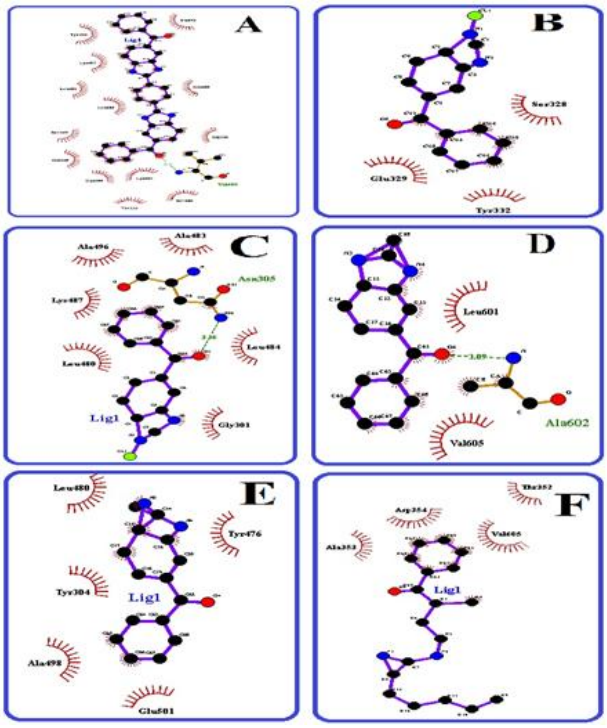

Fig 18: 2D docking study of synthesized BPBB ligand and metal complexes.

2D representation of A)BPBB, B) Fe^{+2} metal complexes, C) Co^{+2} metal complexes, D) Ni^{+2} metal complexes, E) Cu^{+2} metal complexes and F) Zn^{+2} metal complexes with receptor D-fructose-6-phosphate amidotransferase

3.7.3. Antioxidant activity.

Free-radical-scavenging activity using the DPPH method.

The DPPH radical scavenging activity data represented in table 9, fig 20 and fig 20. DPPH solution in methanol gives strong absorbance at 517 nm. If DPPH abstracts a hydrogen radical from an external source, the absorption decreases stoichiometrically depending on the number of electrons or hydrogen atoms [53]. The metal complexes showed significantly higher activity than BPBB, but lower when compared to ascorbic acid (vitamin C) as standard. The Zn^{+2} complex exhibited highly potent scavenging activity almost close to the standard Vitamin-C and Co^{+2} complex and Ni^{+2} also showed better inhibitions activity against free radical and the BPBB and Cu^{+2} showed moderate activity.

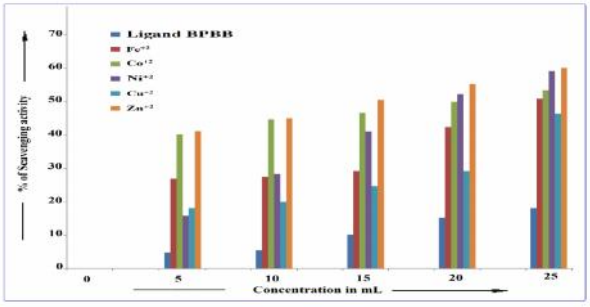

Fig 19: Free-radical-scavenging activity.

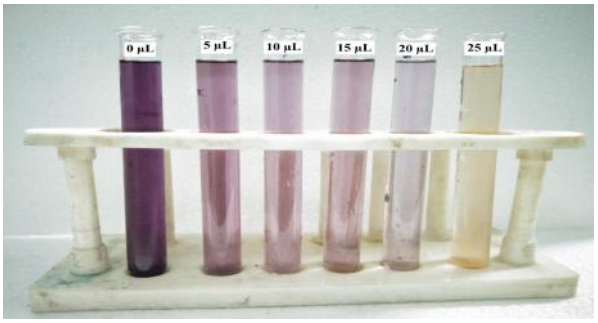

Fig 20: Free-radical-scavenging activity result.

Free-radical-scavenging activity result of Zn^{+2} metal complex using the DPPH method

4. CONCLUSIONS

In the present work, we successfully designed and developed a benzene bridged 1,4-Bis(5-Phenylmethionone-benzimidazole)benzene (BPBB) and its metal complexes. The ligand and their complexes have been characterized by various analytical techniques. ^1H NMR and ^{13}C NMR clearly shows that plane of symmetrical structure of the bis-benzimidazole ligand. IR spectra data indicate the bidentate bonding mode of ligand with 3d metal ions, coordinated through the oxygen atom of carbonyl carbon and imine nitrogen atoms of benzimidazole ring.

Table 9: Scavenging activity.

Concentration in µL	Ligand	[Fe $(BPBB)_2Cl_2$]	[Co $(BPBB)_2Cl_2$]	[Ni $(BPBB)_2Cl_2$]	[Cu $(BPBB)_2Cl_2$]	[$ZnCl_2$ (BPBB)]	Ascorbic acid
0	-	-	-	-	-	-	-
5	04.83±0.05	26.95 ±0.01	40.24 ±0.25	15.85 ±0.05	18.08 ±0.30	41.13± 0.22	49.10±0.25
10	05.51±0.12	27.48 ±0.39	44.68 ±0.26	28.33 ±0.21	20.03 ±0.08	45.03± 0.03	55.23±0.02
15	10.10±0.22	29.25 ±0.14	46.63 ±0.35	41.04 ±0.17	24.64 ±0.24	50.53± 0.17	62.53±0.15

20	**15.24±0.06**	**42.37 ±0.02**	**50.00 ±0.03**	**52.23 ±0.30**	**29.25 ±0.16**	**55.31± 0.20**	**70.31±0.04**
25	**18.08±0.14**	**50.88 ±0.18**	**53.36 ±0.10**	**57.94 ±0.25**	**46.45 ±0.01**	**60.10± 0.13**	**78.10±0.08**

The electronic absorption spectra suggest the octahedron geometry of the Fe, Co, Ni and Cu metal complexes. The tetrahedral geometrical arrangement of Zn(II) complex can be confirmed by mass spectra of the complex. The TGA/DTA data indicate stepwise degradation and from this, the kinetic parameters were evaluated. The obtained analytical techniques results are in good agreement with the proposed structure. Their antimicrobial activity were evaluated on three different concentration of compounds, in which Zn(II) complex performs good activity against both bacterial and fungal salines. The MIC studies of both BPBB and metal complexes against bacterial and fungal strains at different concentrations ware evaluated. The Co(II) and Zn(II) complexes showed potential MIC values against bacterial and fungal strains respectively. Molecular docking studies reveals that Zn(II) complex have comparatively least binding scores as compared glucosamine-6-phosphate synthase (EC 2.6.1.16) as target site receptor may be considered as a potent antimicrobial agent. The complexes showed significant antioxidant activity compared to uncoordinated ligand. Among the studied complexes, zinc complex exhibited promising antioxidant activity as compared with other complexes.

5. ACKNOWLEDGEMENTS

The authors are thankful to the Principal and the Department of Chemistry and bio chemistry, Sahyadri Science College, Shimoga, Karnataka, India, for providing the necessary research facilities. We are also grateful to Indian Institute of Scientific Education & Research, Pune (IISER), Sophisticated Analytical Instruments Facility, Cochin University, Cochin, Kerala, India, MIT Manipal and IISC Bengaluru for providing analytical and spectral data.

6. REFERENCES

1. Nadeem Siddiquia, Priya Ahujaa, Waquar Ahsana, Pandeyab SN, Shamsher Alama M: Thiadiazoles: Progress Report on Biological Activities. J Chem Pharm Rese 2009; 1(1):19-30
2. Bahaa GM, Abdel AM, Hussein M: Synthesis of 1-acyl-2-alkylthio-1,2,4-triazolobenzimidazoles with antifungal, anti-inflammatory and analgesic effects. Acta Pharm. 2006; 56: 31.
3. Achar KC, Hosamani KM, Seetharamareddy HR: In-vivo analgesic and anti-inflammatory activities of newly synthesized benzimidazole derivatives. Eur J Med Chem 2010; 45(5): 2048–2054.
4. Khan SA, Nandan AM: 2-substituted benzimidazoles as anti-inflammatory and analgesic agents. Ind. J. Het. Chem 1997; 7: 55-58.
5. Bariwal JB, Shah AK, Kathiravan MK, Somani RS, Jagtap JR, Jain KS: Synthesis and antiulcer activity of novel Pyrimidylthiomethyl benzimidazole and Pyrimidylsulfinylmethyl benzimidazole as potential reversible proton pump inhibitors. Indian J. Pharm. Educ. Res 2008; 43: 225-231.
6. Canan KUS: Synthesis of some new benzimidazole carbamate derivatives for evaluation of antifungal activity. Turk J Chem 2003; 27(1): 35-39.
7. Chhonker YS, Veenu B, Hasim SR, Niranjan Kaushik , Devendra Kumar, Pradeep Kumar: Synthesis and Pharmacological Evaluation of Some New 2-Phenyl benzimidazoles Derivatives and their Schiff's Bases. E J Chem 2009; 6 (S1): S342-S346.
8. Pathak D, Siddiqui N, Bhrigu, Bhanupriya, Ahsan W, Alam MS: Scholars Research Library. Der Pharmacia Lettre 2010; 2 (2): 27.
9. Reddy VB, Singla RK, Varadaraj G, Bhatt S, Gautham G: Asian J. Res. Chem 2009; 2 (2): 162.
10. Theodorides VJ, Gyurik RK, Kingsbury WD, Parish RC: Anthelmintic activity of albendazole against liver flukes, tapeworms., lung and gastrointestinal roundworms. Experientia 1976; 32(6): 702-703.
11. Demirayak S, Abu Mohsen U, Cagri Karaburun A: Synthesis and anticancer and anti-HIV testing of some pyrazino[1,2-a]benzimidazole derivatives. Eur. J. Med. Chem 2002; 37(3): 255-260.
12. Vinodkumar R, Vaidya SD, Siva Kumar BV, Bhise UN, Bhirud SB, Mashelkar UC: Synthesis, anti-bacterial, anti-asthmatic and anti-diabetic activities of novel N-substituted-2-(4-phenylethynyl-phenyl)-1H-benzimidazoles and N-substituted 2[4-(4,4- dimethyl-thiochroman-6-yl-ethynyl)-phenyl)-1H-benzimidazoles. Eur J Med Chem 2008; 43(5): 986-995.
13. Yar MS, Abdullah M, Majeed J: In vitro anti-tubercular screening of newly synthesized benzimidazole derivatives. World Acad. Sci. Eng. Technol 2009; 55: 593-599.
14. Zygmunt K, Jacqueline A, Upcroft P, Agata G, Bohdan S, Laudy A: Synthesis, antiprotozoal and antibacterial activity of nitro- and halogeno-substituted benzimidazole derivatives. Acta Biochemia Polinia 2002; 49 (1): 185-195..
15. Bishop BC, Chelton ETJ, Jones AS: The antibacterial activity of some fluorine-containing. Benzimidazoles. Biochem. Pharmacol 1964; 13: 751-754.
16. Habib N, Soliman R, Ashour F, El-Taiebi M : Synthesis and antimicrobial testing of novel oxadiazolylbenzimidazole derivatives. El-Taiebi, *Pharmazie* 1997; 52 : 746-749.
17. Tuncbilek M, Goker H, Ertan R, Eryigit R, Kendi E, Altanlar E: Synthesis and antimicrobial activity of some

new anilino benzimidazoles. Arch. Pharm 1997; 330 (12): 372-376.
18. Goker H, Kus C, Boykin DW, Yildiz S, Altanlar N: Synthesis and antimicrobial activity of some new 2-Phenyl-N-substituted carboxamido-1H- benzimidazole derivatives. Arch. Pharm. 2001; 334: 148-152.
19. Goker H, Kus C, Boykin DW, Yildiz S, Altanlar N: Synthesis of some new 2-substituted-phenyl-1H-benzimidazole-5-carbonitriles and their potent activity against Candida species. Bioorg. Med. Chem 2002; 10 (8): 2589-2596.
20. Pawar NS, Dalal DS, Shimpi SR, Mahulikan PP: Studies of Antimicrobial Activity of N-Alkyl and N-Acyl-2-(4-Thiazolyl)-1H-Benzimidazoles. Eur. J. Pharm Sci 2004; 21: 115-118.
21. Mohammad BG, Hussein MA, Abdel-Alim AA, Hashem M: Synthesis and antimicrobial activity of some new 1-alkyl-2-alkylthio-1,. 2, 4-triazolobenzimidazole derivatives Arch. Pharm. Res 2006: 29 (1): 26-33.
22. Vaidya SD, Kumar BVS, Kumar RV, Bhise UN,Mashelkar UC: Synthesis, anti-bacterial, anti-asthmatic and anti-diabetic activities of novel N-substituted-2-(benzo[d]isoxazol-3-ylmethyl)-1H-benzimidazoles. J. Heterocycl. Chem 2007; 44 : 685-691.
23. Porcari AR, Devivar RV, Kucera LS, Drach JC, Townsend LB: Design, Synthesis, and Antiviral Evaluations of 1-(Substituted benzyl)-2-substituted-5,6-dichlorobenzimidazoles as Nonnucleoside Analogues of 2,5,6-Trichloro-1-(β- d -ribofuranosyl)benzimidazole. Journal of Medicinal Chemistry 1998;41(8):1252–1262.
24. Kumar BV, Reddy VM: Synthesis and biological activities of some new S-. (benzimidazol-2ylmethyl) N-substituted dithiocarbamates and N1-substituted. N4-(benzimidazol-2ylmethyl)sulfanilamides, Indian J. Chem 1985; 24(B):1298-1301.
25. Olin, J.F., [U.S. 3 (1975) 860], *C.A.*, 1975, vol.82, p.155907.
26. Mishra, L., and Kagini, S., *J. Indian Chem*., 1999, vol.76, p.500.
27. Singh J, Grover P, Pathak DP: Synthesis, anticonvulsant activity and comparative QSAR study of some novel 1, 2, 5-trisubstituted benzimidazole derivatives. Acta Pharmaceutica Sciencia 2010; 52: 511–522.
28. Mohamed Mohamed Youssef, Mahmoud Ahmed Amin: Microwave Assisted Synthesis of Some New HeterocyclicSpiro-Derivatives with Potential Antimicrobial and Antioxidant Activity. Molecules 2010; 15: 8827-8840.
29. Farukh Arjmand, Bhawana Mohani, Shamim Ahmad: Synthesis, antibacterial, antifungal activity and interaction of CT-DNA with a new benzimidazole derived Cu(II) complex, Europ J Med Chem 2005; 40: 1103–1110.
30. Wu H, Kong J, Yang Z, Wang X, Shi F, Zhang Y: Copper(II) and manganese(II) picrate complexes with the V-shaped ligand 1,3-bis(1-methylbenzimidazol-2-yl)-2-thiapropane: preparation, structure, DNA-binding properties and antioxidant activities. Trans. Met. Chem 2014; 39: 951-960.
31. Shadia A. Galal, Khaled H. Hegab, Ahmed M. Hashem, Nabil S. Youssef: Synthesis and antitumor activity of novel benzimidazole-5-carboxylic acid derivatives and their transition metal complexes as topoisomerease II inhibitors. Europ J Med Chem. 2010; 45: 5685-5691.
32. Muhammad Khattab, Galal SA, Fatma AF, Ragab, Hoda I, El Diwani: Different synthetic routes to 4-(1H-benzo[d] imidazol-2-yl)aniline. Res Chem Intermed 2013; 39 (7): 2917-2923.
33. Krishnamurthy, G., *Hindawi publishing corporation*., 2012, DOI 10.1155/2013/265107.
34. El-Gammal OA, Mostafa MM: Synthesis, characterization, molecular modeling and antioxidant activity of Girard′s T thiosemicarbazide and its complexes with some transition metal ions. Spectrochimica Acta Part A: Molecular and Biomolecular Spectroscopy. 2014; 127: 530–542.
35. Geary WJ: The use of conductivity measurements in organic solvents for the characterisation of coordination compounds. Coord. Chem. Rev. 1971; 7 (1): 81–122.
36. Nakamoto K: Infrared and Raman Spectra of Inorganic and Coordination Compounds, John Wiley & Sons Inc., 1997.
37. Rabiger DJ, Joullie MM: The Ionization Constants, Ultraviolet and Infrared Spectra of Some Substituted Benzimidazoles. J. Org. Chem. 1964; 29 (2):476–482.
38. Takeuchi H, Harada I: Normal mode analysis of indole ring. Spectrochim Acta A. 1986;42:1069–1078.
39. Mayfield HG, Bull WE, Matsmoto T: J. Chem. Soc. 1971; 2280.
40. Bennet AMA, Foulds GA,. Thornton DA, Watkins GM: The infrared spectra of ethylenediamine complexes *II*. *Tris*-, *bis*- and *mono*-(ethylenediamine) complexes of metal(II) halides. Spectrochim. Acta 1990; 46 (A): 13-22.
41. Niben ML, Percy GC: Infrared Spectra of Some Metal (II) Complexes of 2-Aminomethylpyridine. Spectrosc. Lett. 1977; 10(7): 519-525.
42. Agh-Atabay NM, Basaran Dulger, Fahrettin Gucin: Structural characterization and antimicrobial activity of 1,3-bis(2-benzimidazyl)-2-thiapropane ligand and its Pd(II) and Zn(II) halide complexes. Eur. J. Med. Chem. 2005; 40 (11): 1096-1102.
43. Rahaman F, Mruthyunjayaswamy BHM: Synthesis, spectral characterization, grain size effect, antimicrobial, DNA cleavage and anticancer activities of cobalt(II),

nickel(II), copper(II) and zinc(II) complexes of schiff base. Comp. Met. 2014;31: 88-95.

44. Sreekanth B, Krishnamurthy G, Bhojya Naik HS, Vishnuvardhan TK: Cu(II) and Mn(II) complexes containing macroacyclic ligand: synthesis, DNA binding, and cleavage studies syn, dna binding, and cleavage studies. Nucleos. Nucleot. Nucleic Acids 2012; 31:1-13.
45. (a) Issa RM, Hassanein AA, El-Mehasseb IM, Abed RI, El-Wadoud: UV–vis, IR and ^{1}H NMR spectroscopic studies of some 6-chloro,2-pyridyl hydrazones. Spectrochim. Acta 2006; 65 (1): 206-214.
46. (b) Issa RM, Kamal Y, El-baradie, Nadia A, El-Wakiel: UV/Vis, IR and ^{1}H NMR spectrophotometric studies of some bisazo-dianil compounds based on bis-(hydroxy, formyl) phenylazo phenylene and anthranilic acid. Spectrochim. Acta 2004; 60 (12): 2883-2889.
47. Ashraf A, Siddiqui WA, Akbar J, Mustafa G, Krautscheid H, Ullah N: Metal complexes of benzimidazole derived sulfonamide: synthesis, molecular structures and antimicrobial activity. Inorg. Chimca Acta 2016; 443:179-185.
48. Krishnamurthy G: Synthesis and characterization of ruthenium(III) chloride complexes with some 1,2-disubstituted benzimidazoles and their catalytic activity. Syn Reac. Inorg. Met Org. Nano Metal Chem. 2011; 41: 590-597.
49. Coats AW, Redfern JP: Kinetic parameters from thermogravimetric data. Nature 1964; 20 : 68.
50. Koch AL: Bacterial Wall as Target for Attack. Clin. Microbiol. Rev. 2003; 16 (4): 673-687.
51. Nour T. Abdel Ghani, Mansour AM: Novel palladium (II) and platinum (II) complexes with 1H-benzimidazol-2-ylmethyl-N-(4-bromo-phenyl)-amine: structural studies and anticancer activity. Inorganica Chimica Acta 2011; 373: 249–258.
52. Yadav G, Ganguly S: Structure activity relationship (SAR) study of benzimidazole scaffold for different biological activities: a mini-review. Eur. J. Med. Chem. 2015; 97: 419-443.
53. Patil BS, Krishnamurthy G, Lokesh MR, Shashikumar ND, Bhojya Naik HS, Latthe PR, Manjunath Ghate: Synthesis of some novel 1,2,4-triazole and 1,3,4-oxadiazole derivatives of biological interest. Med Chem Res 2012; 21(11):3327-3928.
54. Harinath Y, Reddy DHK, Kumar BN, Apparao C, Seshaiah K: Synthesis, spectral characterization and antioxidant activity studies of a bidentate Schiff base, 5-methyl thiophene-2-carboxaldehyde-carbohydrazone and its Cd (II), Cu (II), Ni (II) and Zn (II) complexes. Spect Acta Part A: Mole Biom Spect.2013; 101:264–272.

Conflict of Interest: None

Source of Funding: Nil